Communication

Facile Synthesis of Tadpole-like Nanostructures Consisting of Au Heads and Pd Tails

Pedro H. C. Camargo, Yujie Xiong, Li Ji, Jian M. Zuo, and Younan Xia

J. Am. Chem. Soc., **2007**, 129 (50), 15452-15453 • DOI: 10.1021/ja077505a

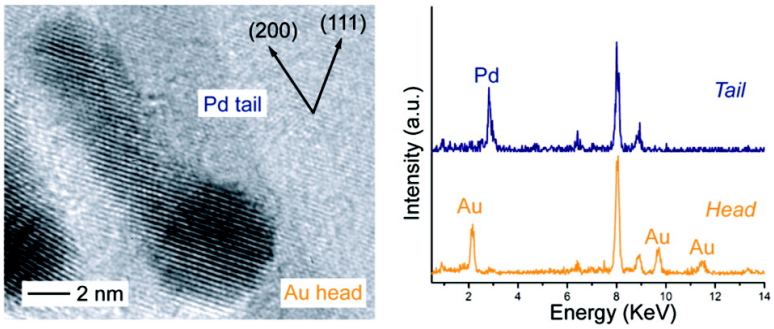

More About This Article

Additional resources and features associated with this article are available within the HTML version:

- Supporting Information
- Links to the 6 articles that cite this article, as of the time of this article download
- Access to high resolution figures
- Links to articles and content related to this article
- Copyright permission to reproduce figures and/or text from this article

View the Full Text HTML

J|A|C|S
COMMUNICATIONS

Published on Web 11/21/2007

Facile Synthesis of Tadpole-like Nanostructures Consisting of Au Heads and Pd Tails

Pedro H. C. Camargo,[†] Yujie Xiong,[†] Li Ji,[‡] Jian M. Zuo,[‡] and Younan Xia*[,†]

Department of Chemistry, University of Washington, Seattle, Washington 98195-1700, and Department of Materials Science and Engineering, University of Illinois at Urbana−Champaign, Urbana, Illinois 61801

Received September 28, 2007; E-mail: xia@biomed.wustl.edu

Hybridization provides an effective strategy for enhancing the functionality of materials.[1] It is also possible to tune the electronic and optical properties of nanoparticles by forming a hybrid system.[2] Palladium serves as a major catalyst in many industrial applications.[3] It has been shown that incorporation of Au into Pd nanoparticles can reduce the material cost while enhancing their catalytic activity, selectivity, and stability.[4] Here we report the synthesis of Pd−Au hybrid nanostructures in a tadpole shape, with the head being a Au nanoparticle and the tail being a Pd nanorod. The synthesis is based upon the galvanic replacement reaction between single-crystal Pd nanorods and $AuCl_4^-$ ions. Different from previous systems that involved Ag-based templates and $AuCl_4^-$ ions,[5] the Au atoms resulting from the galvanic reaction did not coat the entire surface of a Pd nanorod to generate a core-sheath or hollow structure. Instead, the nucleation and deposition of Au was localized to the end(s) of a Pd nanorod, leading to the formation of a Pd−Au tadpole.

Figure 1A shows a TEM image of the initial Pd nanorods that had an octagonal cross section, with the side surface enclosed by a mix of {100} and {110} facets. They had an average diameter of 4.0 ± 0.3 nm and length of 17.4 ± 2.4 nm (78% of them were rods). The nanorods were synthesized by reducing $PdCl_4^{2-}$ ions with ethylene glycol in water in the presence of poly(vinyl pyrrolidone) (PVP) and Br^- ions.[6] According to our proposed mechanism, cuboctahedral seeds were formed in the nucleation stage, whose surfaces were passivated by Br^- ions.[7] Oxidative etching due to the presence of oxygen (from air) and chloride (from $PdCl_4^{2-}$) could break the cubic symmetry of a seed, leading to the formation of an octagonal nanorod.[8]

Panels B−D of Figure 1 show TEM images of the products after the Pd nanorods had reacted with different volumes of 0.4 mM $HAuCl_4$. Specifically, after the addition of 1 mL of $HAuCl_4$ (Figure 1B), both ends of each Pd nanorod started to be enlarged and became rounded due to the deposition of Au via the following reaction:

$$3Pd_{(s)} + 2AuCl_4^-{}_{(aq)} \rightarrow 3Pd^{2+}{}_{(aq)} + 2Au_{(s)} + 8Cl^-{}_{(aq)} \qquad (1)$$

The nanorods shown in Figure 1B had an average diameter of 3.5 ± 0.3 nm and length of 18.4 ± 2.9 nm (75% of them were rods). It is important to note that Pd oxidation can occur from any place on the entire surface of a nanorod, including the {100} and {110} side faces and the {100} ends. However, Au deposition only occurs at the ends (Figure S1). This can be attributed to the fact that the electrons resulting from the oxidation of Pd tend to be separated as far as possible (in this case, to the ends of a nanorod) due to a strong repulsion between them. Pd is also a good conductor, in which electrons can migrate freely.

As more $HAuCl_4$ was added, more Pd would be dissolved from the nanorod accompanying the further deposition of Au onto both ends. Interestingly, a transition from two-end to one-end growth was observed, producing a Pd−Au tadpole consisting of a Au head and a Pd tail (Figure 1C). In this case, Ostwald ripening occurred for each nanostructure that shifted Au from one end to the other. This behavior was first proposed for the growth of Au tips on CdSe nanorods and can be understood as the following:[9a] as the Au heads became bigger, their size difference also increased to create a driving force for Ostwald ripening.[9] The presence of a Pd segment between the two Au heads greatly facilitates the ripening process as Pd is a good conductor for electrons. After further addition of $HAuCl_4$ (Figure 1D), more Pd consumption from the rods caused deposition of more Au at the preformed Au heads, increasing their diameter to 11 nm. At the same time, it can be observed that the width and length of the Pd tails in Figure 1C and 1D (W/L = 3.4 ± 0.4/11.9 ± 1.8 and 2.9 ± 0.4/11.6 ± 2.5 nm, respectively; 75% of them were rods) were both reduced relative to the initial Pd nanorods (4.0 and 17.4 nm).

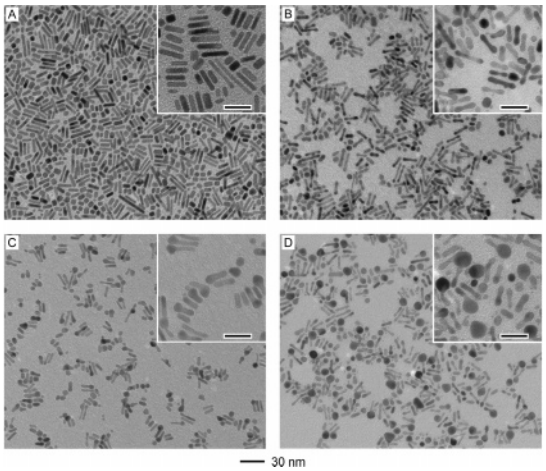

Figure 1. TEM images of (A) Pd nanorods and (B−D) samples that were obtained by titrating the Pd nanorods with different volumes of 0.4 mM $HAuCl_4$ solution: (B) 1, (C) 2, and (D) 4 mL. The scale bars in the insets correspond to 20 nm.

When an excess amount of $HAuCl_4$ was introduced, the Pd−Au tadpoles were dismantled into smaller/shorter Pd nanorods and spherical Au nanoparticles (Figure S2). At this point, even though the amount of $HAuCl_4$ added was enough to consume all the Pd from the nanorods, complete Pd oxidation was not observed. This can be attributed to the coverage of side surface by Au atoms at a late stage of the reaction, preventing the Pd nanorods from further oxidation. This is supported by STEM/EDS data (see discussion below), in which a small content of Au was detected along the Pd tail. It is worth pointing out that the samples shown in Figure 1C,D appear to present fewer Au heads than Pd tails. It is possible that, after the transition from two-end to one-end growth, Ostwald ripening of the Au tips continued to take place resulting in fewer, large Au heads. It is also possible that each Pd nanorod was broken

[†] University of Washington.
[‡] University of Illinois at Urbana−Champaign.

10.1021/ja077505a CCC: $37.00

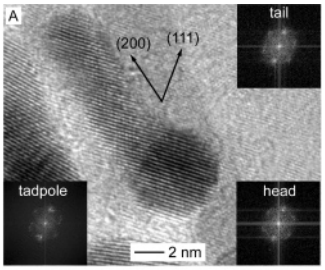

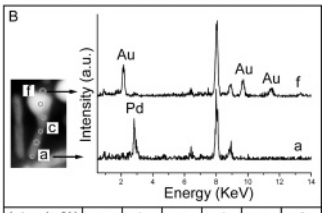

(atomic %)	a	b	c	d	e	f
Pd	97.9	90.5	93.0	64.2	6.9	6.2
Au	2.1	9.5	7.0	35.8	93.1	93.8

Figure 2. (A) High-resolution TEM image recorded along [110] for the Pd−Au tadpoles shown in Figure 1C. The insets show FFT operations for the Pd tail, Au head, and for the overall tadpole. In all cases, a hexagonal pattern of six points is observed, as expected for both *fcc* Au and Pd in the [011] beam direction. (B) STEM/EDS analysis on six different sites along the Pd−Au tadpole (a−f), as marked on the DF STEM image. The table shows the EDS atomic percentages for Pd and Au obtained for each position. The EDS spectra for points a and f are also included.

into several segments to double or triple its number. Figure S3 shows the UV−vis spectra taken from the solution at various stages of the reaction, clearly showing the evolution of a surface-localized plasmon resonance (LSPR) peak associated with the Au nanoparticles. Because the LSPR peak of Pd nanorods (i.e., tails) is located in the UV region, it is expected that the coupling between these two SPR peaks is relatively weak and can be neglected.

Figure 2A shows a high-resolution TEM image recorded along the [110] axis (with respect to the Pd tail). It can be observed that the hybrid nanostructure is a piece of single crystal. Due to a close matching between the {111} lattice spacings of Au and Pd (4% mismatch), the Au atoms could nucleate and grow epitaxially from the end faces of a Pd nanorod along the [100] direction, producing parallel fringes between the tail and the spherical head. The {111} fringes show a period of 2.24 and 2.36 Å, as expected for *fcc* Pd and Au, respectively. We also performed a STEM/EDS line scanning analysis to reveal the compositional variation along the long axis of the tadpole-shaped nanostructure (Figure 2B). As illustrated on the dark-field STEM image, the percentages of Pd and Au were determined for six different sites, a to f, where a is located at the bottom of the tail and f at the top of the head. The results show that the tail (a to c) is indeed composed mostly of Pd. The atomic percentage for Au was 2.1, 9.5, and 7.0%, respectively. The low percentages of Au in the tail can probably be attributed to the surface diffusion of Au along the Pd tail. This result also explains the incomplete oxidation of Pd observed at later stages of the galvanic reaction. Site d, which is from the region connecting the tail to the head, contains both Pd and Au (64.8 and 36.2%, respectively). Finally, the atomic percentages for sites e and f confirm that the heads contain mostly Au (∼93%). Figure S4 summarizes all major steps involved in the localized deposition of Au as a result of the galvanic replacement reaction.

In summary, we have demonstrated the synthesis of a new type of hybrid nanostructure in the tadpole shape consisting of a Au head and a Pd tail. The formation of such a morphology involved a localized galvanic replacement mechanism. In the earlier stages of the reaction, localized deposition of Au onto both ends of a rod was observed because the electrons tend to be pushed to the ends of the rod as a result of the repulsive forces. At a later stage, a transition from two-end to one-end growth occurred as a result of Ostwald ripening, leading to the formation of a Pd−Au tadpole composed of a Au head and a Pd tail. It is worth pointing out that this localized deposition of Au is unique for Pd nanorods. No such phase segregation was observed when Pd nanoparticles were used in place of the rods. We note that a similar structure was also observed by Wetz et al.[10] for the galvanic reaction between Co nanorods and Au compounds. However, these authors did not provide detailed elemental analysis on each hybrid nanostructure, did not observe the transition from two-end to one-end growth, and did not recognize the importance of rod shape in promoting the localized deposition of Au. It is expected that these Pd−Au tadpoles, combining the properties from both Pd nanorods and Au nanoparticles, may find use in catalysis and LSPR sensing owing to the exceptional sensitivity of Pd toward H_2. This method can also be extended to other metals, such as Pt, to produce a variety of Pd-based hybrid nanostructures.

Acknowledgment. This work was supported in part by ACS (PRF-44353-AC10) and a Director's Pioneer Award from NIH (5DP1OD000798). P.H.C.C. has been partially supported by the Fulbright Program and the Brazilian Ministry of Education (CAPES). J.M.Z. and L.J. were supported by DOE (DEFG02-01ER45923). Part of the electron microscopy work was carried out at the Center for Microanalysis of Materials at the Frederick Seitz Materials Research Laboratory, which is partially supported by DOE under Grant DEFG02-91-ER45439.

Supporting Information Available: Experimental procedures, TEM images, UV−vis spectra, and schematic illustrating the formation of a Pd−Au tadpole. This material is available free of charge via the Internet at http://pubs.acs.org.

References

(1) See, for example: (a) Xiang, Y.; Wu, X.; Liu, D.; Jiang, X.; Chu, X.; Li, Z.; Ma, L.; Zhou, W.; Xie, S. *Nano Lett.* **2006**, *6*, 2290. (b) Gao, J. H.; Liang, G. L.; Zhang, B.; Kuang, Y.; Zhang, X. X.; Xu, B. *J. Am. Chem. Soc.* **2007**, *129*, 1428. (c) Gao, J. H.; Zhang, B.; Gao, Y.; Pan, Y.; Zhang, X. X.; Xu, B. *J. Am. Chem. Soc.* **2007**, *129*, 11928. (d) Maksimuk, S.; Yang, S. C.; Peng, Z. M.; Yang, H. *J. Am. Chem. Soc.* **2007**, *129*, 8694.

(2) (a) Xiong, Y.; Wiley, B.; Chen, J.; Li, Z.-Y.; Yin, Y.; Xia, Y. *Angew. Chem., Int. Ed.* **2005**, *44*, 7913. (b) Xiong, Y.; McLellan, J. M.; Chen, J.; Yin, Y.; Li, Z.-Y.; Xia, Y. *J. Am. Chem. Soc.* **2005**, *127*, 17118. (c) Xiong, Y.; Chen, J.; Wiley, B.; Xia, Y.; Yin, Y.; Li, Z.-Y. *Nano Lett.* **2005**, *5*, 1237. (d) Xu, Z.; Hou, Y.; Sun, S. *J. Am. Chem. Soc.* **2007**, *129*, 8698.

(3) (a) Nishihata, Y.; Mizuki, J.; Akao, T.; Tanaka, H.; Uenishi, M.; Kimura, M.; Okamoto, T.; Hamada, N. *Nature* **2002**, *418*, 164. (b) Trzeciak, A. M.; Ziółkowski, J. J. *Coord. Chem. Rev.* **2007**, *251*, 1281.

(4) See, for example: (a) Chen, M.; Kumar, D.; Yi, C.-W.; Goodman, D. W. *Science* **2005**, *310*, 291. (b) Enache, D. A.; Edwards, J. K.; Landon, P.; Solsona-Espriu, B.; Carley, A. F.; Herzing, A. A.; Watanabe, M.; Kiely, C. J.; Knight, D. W.; Hutchings, G. J. *Science*, **2006**, *311*, 362. (c) Ferrer, D.; Torres-Castro, A.; Gao, X.; Sepúlveda-Guzmán, S.; Ortiz-Méndez, U.; José-Yacamán, M. *Nano Lett.* **2007**, *7*, 1701.

(5) See, for example: (a) Sun, Y.; Xia Y. *Science* **2002**, *298*, 2176. (b) Chen, J.; Wiley, B.; McLellan, J.; Xiong, Y.; Li, Z.-Y.; Xia, Y. *Nano Lett.* **2005**, *5*, 2058−2062. (c) Chen, J.; McLellan, J. M.; Siekkinen, A.; Xiong, Y.; Li, Z.-Y.; Xia, Y. *J. Am. Chem. Soc.* **2006**, *128*, 14776. (d) Lu, X.; Tuan, H.-Y.; Chen, J.; Li, Z.-Y.; Korgel, B. A.; Xia, Y. *J. Am. Chem. Soc.* **2007**, *129*, 1733.

(6) Xiong, Y.; Cai, H.; Wiley, B. J.; Wang, J.; Kim, M. J.; Xia, Y. *J. Am. Chem. Soc.* **2007**, *129*, 3665.

(7) (a) Lucas, C. A.; Marković, N. M.; Ross, P. N. *Phys. Rev. B* **1997**, *55*, 7964. (b) Zou, S.; Gao, X.; Weaver, M. J. *Surf. Sci.* **2000**, *452*, 44.

(8) (a) Newman, R. C.; Sieradzki, K. *Science* **1994**, *263*, 1708. (b) Scully, J. C. *The Fundamentals of Corrosion*, 3rd ed.; Pergamon Press: Oxford, New York, 1990; pp 1−57. (c) Tsung, C.-K.; Kou, X.; Shi, Q.; Zhang, J.; Yeung, M. H.; Wang, J.; Stucky, G. D. *J. Am. Chem. Soc.* **2006**, *128*, 5352. (d) Sun, Y.; Xia, Y. *J. Am. Chem. Soc.* **2004**, *126*, 3892.

(9) (a) Mokari, T.; Sztrum, C. G.; Salant, A.; Rabani, E.; Banin, U. *Nat. Mater.* **2005**, *4*, 855. (b) Saunders, A. E.; Popov, I.; Banin U. *J. Phys. Chem. B* **2006**, *110*, 25421. (c) Redmond, P. L.; Hallock, A. J.; Brus, L. E. *Nano Lett.* **2005**, *5*, 131.

(10) Wetz, F.; Soulantica, K.; Falqui, A.; Respaud, M.; Snoeck, E.; Chaudret, B. *Angew. Chem.* **2007**, *119*, 7209.

JA077505A